plasma

MDPI

Review

Flexible Cold Atmospheric Plasma Jet Sources

Carles Corbella *, Sabine Portal and Michael Keidar

Department of Mechanical and Aerospace Engineering, George Washington University, Washington, DC 20052, USA

* Correspondence: ccorberoc@gwu.edu

Abstract: The properties of non-thermal atmospheric pressure plasma jets (APPJs) make them suitable for industrial and biomedical applications. They show many advantages when it comes to local and precise surface treatments, and there is interest in upgrading their performance for irradiation on large areas and uneven surfaces. The generation of charged species (electrons and ions) and reactive species (radicals), together with emitted UV photons, enables a rich plasma chemistry that should be uniform on arbitrary sample profiles. Lateral gradients in plasma parameters from multi-jets should, therefore, be minimized and addressed by means of plasma monitoring techniques, such as electrical diagnostics and optical emission spectroscopy analysis (OES). This article briefly reviews the main strategies adopted to build morphing APPJ arrays and ultra-flexible and long tubes to project cold plasma jets. Basic aspects, such as inter-jet interactions and nozzle shape, have also been discussed, as well as potential applications in the fields of polymer processing and plasma medicine.

Keywords: atmospheric pressure plasma jet; multi-jet interaction; flexible nozzles; morphing sources

1. Introduction

A non-thermal atmospheric pressure plasma jet (APPJ) is the afterglow from a dielectric barrier discharge (DBD) projected into ambient air [1,2]. The flow requires a noble gas or an admixture with reactive gases. The elementary parts are streamers, which consist of dipolar charged structures propagating between anode and cathode. The flowing of guided streamers out of the DBD region conform the plasma column, which transits from filamentary to a diffuse homogeneous mode, typically when a set of adjacent streamers overlap [3].

The portability and cost-effective characteristics of APPJ sources make them very attractive for many uses; from material synthesis, surface modification and/or functionalization, through to gas treatments, and biomedical applications. The latter discipline has been a popular topic in both plasma physics and medical device development [4–7]. In particular, the adoption of APPJ treatments to address cancer therapy via selective killing of cancer cells has been a breakthrough in plasma science and technology, which has enabled strong synergies between electrical engineers and healthcare laboratories [7]. Although plasma cancer therapy is still a young discipline, there is common agreement that UV radiation and radicals generated in the mixture of a free jet with air, such as reactive oxygen and nitrogen species (RONS), are associated with the successful performance of plasma jets in wound healing and tumor degradation.

There has been substantial progress towards the understanding of fundamental mechanisms in plasma–biomaterials interactions. However, a pending issue is the mechanical adaptation of plasma sources to the targeted surface. The classical setup in APPJ instrumentation is based on a pen-shape device, which, once fed with electrical power and gas supply, provides a needle-like discharge with millimetric side range [8]. This is the adequate geometry for local treatments, and its use on extended areas demands programming scanning routines and/or the assembly of several parallel nozzles to provide a multi-jet outcome. Accommodation of plasma sources on surfaces showing uneven topology has

check for updates

Citation: Corbella, C.; Portal, S.; Keidar, M. Flexible Cold Atmospheric Plasma Jet Sources. *Plasma* **2023**, *6*, 72–88. https://doi.org/10.3390/plasma6010007

Academic Editor: Andrey Starikovskiy

Received: 1 February 2023
Revised: 13 February 2023
Accepted: 14 February 2023
Published: 16 February 2023

been achieved so far by designing large-area sources based on dielectric barrier discharge (DBD). Paper-based plasma sanitizers, knitted warfare gadgets, and low-power flexible DBD sources summarize the state-of-the-art equipment in flexible plasma sources for large-area treatments [9–12].

It would be desirable to upgrade APPJ technology to make it available for uniform treatments over large areas. An important advantage compared with flexible DBD sources is a better control over plasma chemistry and the option of modifying nozzle-sample distances as per required treatment [13]. Figure 1a shows the main configurations of atmospheric plasma sources for surface modification [14]. The highlighted APPJ column shows the main charged and reactive species coexisting with the primary gas source, typically helium or argon. Maho et al. prepared plasma multi-jet sources for skin treatment, as shown in Figure 1b [15]. However, this configuration does not guarantee homogeneous influx of plasma species onto the irradiated area. The persisting issue is how to improve the uniformity of APPJ treatments over extended surfaces showing arbitrary topography, which is only possible by means of deformable plasma jet arrays or nozzles compliant with target features, such as asperities, trenches, elbows, or holes. This article briefly reviews the main efforts in this respect.

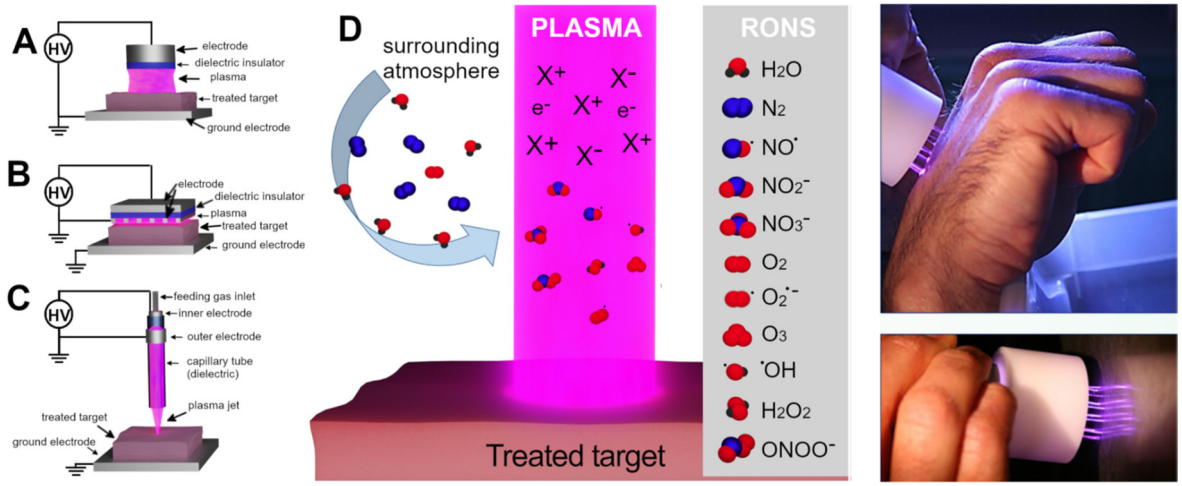

Figure 1. (**a**) Typical configurations of non-thermal atmospheric plasma sources facing a target comprise floating-electrode DBD (A), DBD surface plasma (B), and APPJ source (C). Schematic of an APPJ column (D) together with the generated charged species, and reactive oxygen and nitrogen species or RONS. Reproduced from [14]. Published by Elsevier under the Creative Commons CC-BY-NC-ND license. (**b**) Images of a plasma multi-jet source aimed at skin treatment. Reprinted/adapted with permission from Ref. [15]. Copyright 2017, Elsevier GmbH.

2. Extended- and Multi-Jet Devices

The fabrication of flexible APPJ devices demands an optimal arrangement of the plasma jet nozzles. Either having sources designed in multi-jet arrays or in special nozzle geometries, one should expect plasma systems operating with important interaction issues and performance depending on the coupling at the plasma-sample interface.

2.1. Multi-Jet Interactions

An important aspect to consider when designing APPJ sources with multi-jet arrangement is the nature of interactions between adjacent plasma plumes. As concluded from experimental and computational studies, the four key aspects of technological relevance are the discharge voltage waveform (pulsed vs. sinusoidal AC), timing of each jet, gas flow rate (1–10 lpm), and inter-nozzle distance (few mms) [16–19]. Two main interactions govern the trajectories of multi-jets: hydrodynamic (attractive) and electromagnetic (repulsive).

Figure 2 shows a typical setup to study the optical and electrical characteristics of plasma multi-jets [20]. Here, we only consider free jets. The presence of a target material coupled to the multi-APPJ requires a separate analysis [21]. Moreover, the memory effect on the surface induced by leftover charges from jet interaction substantially enhances the scenario complexity [22].

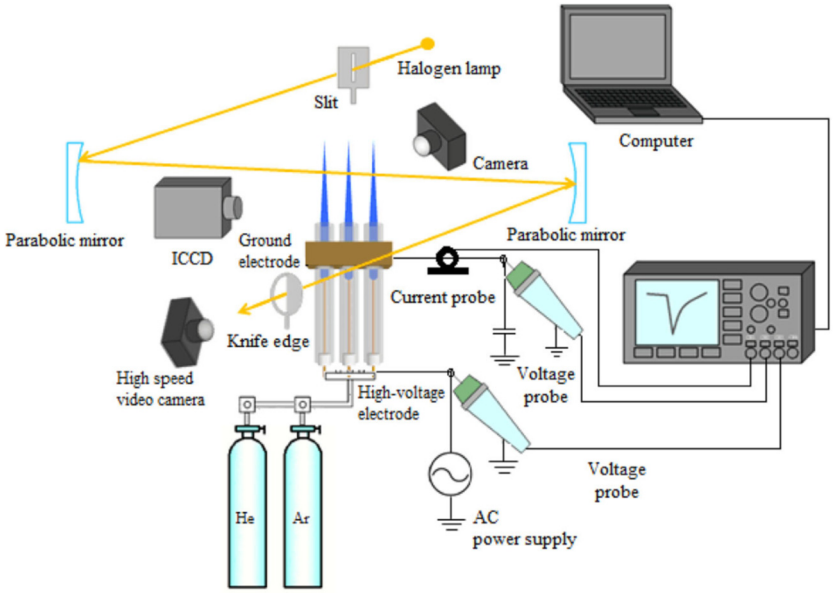

Figure 2. Scheme of an experimental setup prepared for the optical and electrical characterizations of multi-APPJs and associated gas streams. In this setup, both He and Ar APPJs were studied by measuring signal waveforms and obtaining Schlieren images of the plasma plume fluid dynamics. Reprinted/adapted with permission from Ref. [20]. Copyright 2017, WILEY-VCH Verlag GmbH & Co.

Figure 3 shows optical images of a 3-APPJ array along with the corresponding density contrast images obtained by Schlieren imaging [23]. All scenarios evidence multi-jet divergence, whose characteristic angle is larger for the optical emission image due to electrostatic repulsion between the bright plumes. The increase in the divergence angle is observed for lower flow rates and larger voltages. Turbulence phenomena are connected to higher voltages and gas fluxes, which can be explained by the linear dependence of Reynolds number with the gas linear velocity [24]. The use of heavier gases (e.g., Ar vs. He) diminishes the divergence angle due to the larger inertia of heavy plasma atoms [20].

The choice of whether supplying sinusoidal AC voltage or pulsed DC rectangular voltage waveforms, along with the set amplitude and frequency, determines the spatial charge density of each single plasma jet. Naturally, a larger accumulation of spatial charges enhances repulsive interaction between adjacent plumes due to an increase in the jet potential, thereby contributing to jet deflection [18,19]. This deflection is ultimately caused by the electrostatic repulsion existing between guided ionization waves or plasma "bullets", which are the APPJ elementary constituents, and are detectable by high-speed imaging, such as the ICCD technique [25,26]. Such repulsion can be modified by conveniently synchronizing the voltage signal supplied to each jet, which in turn affects the time of flight of the associated bullets. Indeed, Cho et al. showed that the interaction potential in a crossed-flow two-plasma beam could be tuned by selecting the same or opposed polarities of the interacting jets (incidence angle: 90 degrees) [27].

In contrast with electrical interaction, when the hydrodynamic interaction becomes dominant, the multi-jet system tends to converge into a central jet due to inter-jet attractive forces, which compensate for the electrostatic repulsion barrier. The boundary layer of air formed between freely expanding neighboring jets can become very thin, and, in the

limit of close-packed nozzles, such layer can vanish so that adjacent jets merge into a more intense unified plasma column. Fang et al. illustrated this situation by forming one very bright jet out of the merging of all single-participating plasma plumes [28]. In summary, deviations from a straight, collimated multi-jet are expected from the combined hydrodynamic and electrostatic characters of the fluid system. The question of which interaction dominates depends on the specific APPJ setup and operating conditions. Hence, APPJ source parameters need to be adjusted if the electrostatic and hydrodynamic effects appear unbalanced and a collimated jet bundle is required.

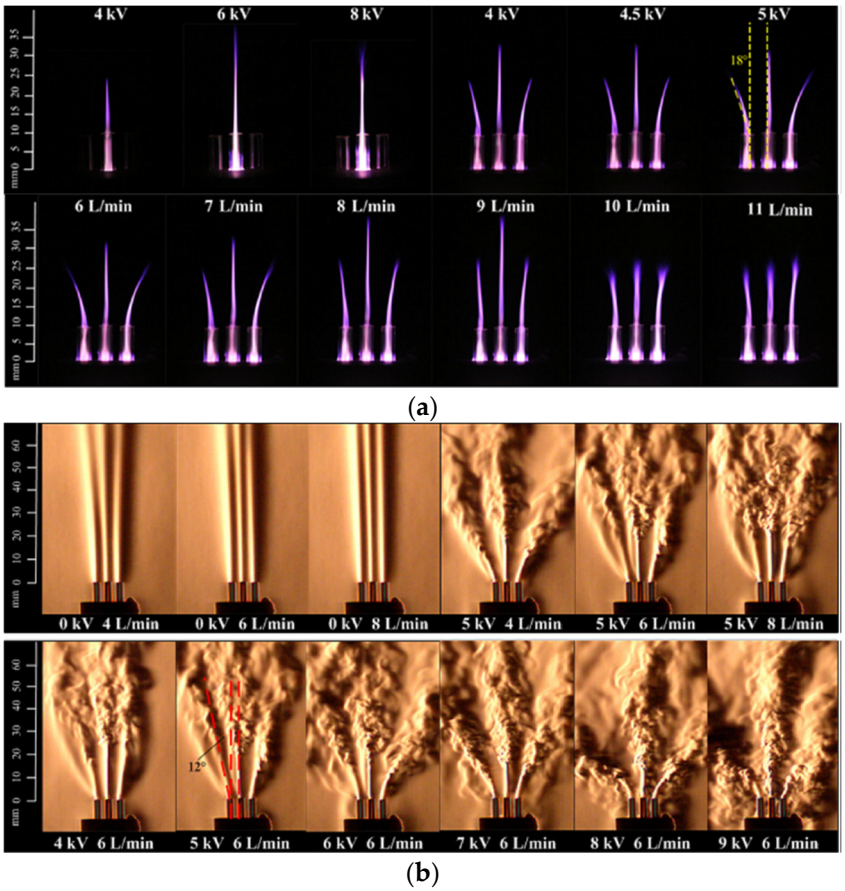

Figure 3. (**a**) Optical images of single- and three-jet arrays at different applied AC voltages and He flow rates. The jet axial separation is around 5 mm in an asymmetric cross-field APPJ setup (needle-to-ring electrodes). (**b**) Corresponding Schlieren images of the APPJ array. Divergence angles are indicated. Reprinted/adapted with permission from Ref. [23]. Copyright 2017, Authors.

2.2. APPJ Nozzle Geometries

Besides inter-jet interactions, the shape of the APPJ nozzle is a subject of interest in the design of flexible plasma jet sources. In general, the orifice from which an APPJ flows to open air is cylindrical with a mm-sized diameter. This is the case for the channels used to design atmospheric microplasma jet sources [29]. Micro-APPJs are commonly used in plasma chemistry research [30,31], and they serve as inspiration for microfluidic plasmas, which is being consolidated as a research line [32].

Alternatives to cylindric apertures are nozzles manufactured with a horn-like shape. Although studies on deformable APPJ nozzles in operando have not yet been reported, Castro et al. have characterized the performance of different horn-like nozzles emitting plasma jets with comparable parameters [33]. In that study, they concluded that the modified area of a polymer surface (wettability and roughness) systematically exceeds the optically visible interaction area. This result is explained by the presence of non-emitting reactive species in the vicinity of the APPJ interaction zone [34]. Figure 4a shows one of the

conical jets with the plasma volume adapted to the object being treated. Another nozzle shape worthy of exploration is the rectangular or slit aperture, which provides plasma afterglows in 2D-like laminar form. Planar APPJs have been explored and show potential applications requiring selected-area plasma processes (Figure 4b) [35,36]. The construction of flexible APPJ devices with variable nozzle shapes will be a valuable milestone in cold plasma applications.

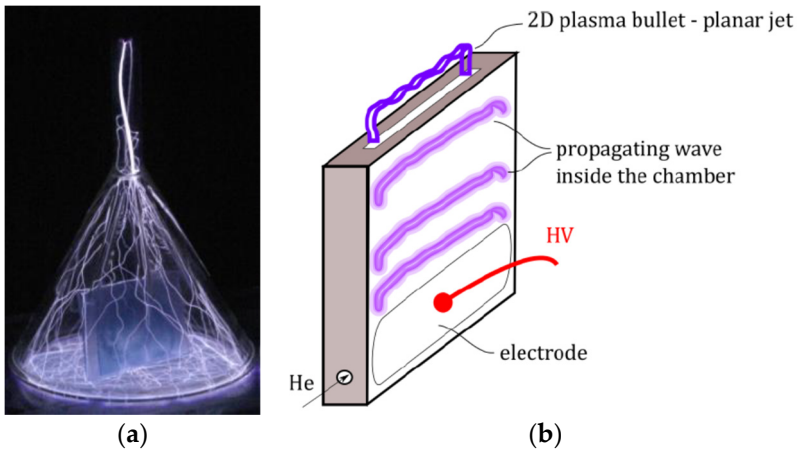

Figure 4. (**a**) Cone-shaped nozzle covering an APPJ-treated vertical object and suppression of air mixing. Nozzle diameter: 64 mm; exposure time: 1.7 ms. Reprinted/adapted with permission from Ref. [34]. Copyright 2018, Elsevier B.V. (**b**) Sketch of a planar APPJ setup. Reproduced from [35]. Published by arXiv.org under a non-exclusive license.

3. Morphing APPJ Arrays

As pointed out in the introduction, many efforts have been made in the construction of flexible plasma source prototypes that operate in ambient air conditions. Some groups mimicked plasma-jet configurations by designing linear arrays of biased pins adaptable to different substrate geometries [37,38]. Nevertheless, not many authors have reported the design and operation of flexible atmospheric plasma multi-jet sources with an independent control over primary gas and its flow rate.

3.1. Close-Packed Microplasma Multijet Arrays

Ma et al. reported an early approach to a plasma multi-jet source made of a flexible material [39]. The body of the source consisted of a molded silicon block with inserted thin rods acting as electrodes, which were biased by a 20 kHz-AC signal at the kV range amplitude. The separation between rods, inter-nozzle distance, and microchannel size were all of the order of 1 mm or less. Hence, sub-millimetric nozzles enabled the production of close-packed collimated micro-APPJs in a square matrix configuration, which ranged from 2 × 2 up to 8 × 8 [40]. Up to three rods in parallel arrangement were inserted across the microchannels direction, as shown in Figure 5a. This disposition is appropriate to separately modulate the energy and length of different arrays of plasma plumes by applying the appropriate voltage values at selected electrodes. Figure 5b shows the range of discharge voltage and the current associated with this setup. The source characterization was completed by optical emission spectroscopy (OES) diagnostics, showing the dominant species in the different positions of the discharge: He, as a primary gas, was relevant within the DBD source region, while a rich profile of nitrogen lines dominated in open air. A helium back pressure of up to 800 Torr was exerted. No jet–jet interaction was observable. Finally, this source successfully reduced burn wound size and sterilized drink water [41,42], thereby validating its performance as an efficient healing and bactericide tool.

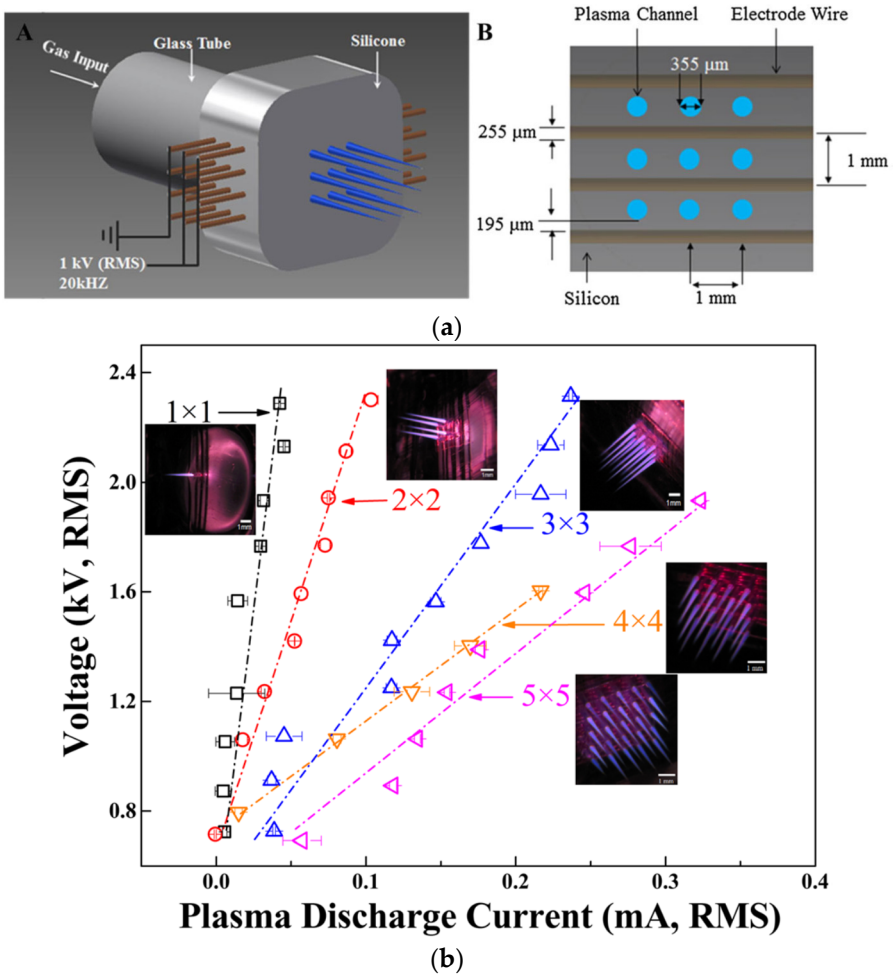

Figure 5. (**a**) Schematic representation of the close-packed microplasma multi-jet source fabricated using a flexible silicone structure. The general view (**A**) and front view (**B**) show the nozzle arrangement with relevant distances. (**b**) V-I characteristics of different micro-APPJ square matrices. Reprinted/adapted with permission from Ref. [41]. Copyright 2015, John Wiley & Sons, Ltd.

The production of reactive plasma species based in oxygen and nitrogen formed near the treated sample is enhanced thanks to the interaction of multiple plasma plumes with the surrounding air. OES spectra depicted in Figure 6a show how RONS density dominates over helium atoms and metastables in the afterglow region in the case of a 3 × 3 microplasma array. The medical therapy capabilities of the microplasma jet array have been demonstrated by treating burn wounds in animal rat models [41]. The plasma plume array treatment promoted a burn size reduction down to 20% of the original size in 2 weeks, whereas the control sample only decreased to 80% of its original size (Figure 6b). It was concluded from the tissue histology that the healing process is accelerated through the regulation of anti-inflammatory processing. However, more detailed analysis of gene expression mechanisms, e.g., via tracking mRNA expressions of inflammatory markers, is pending to complete the study.

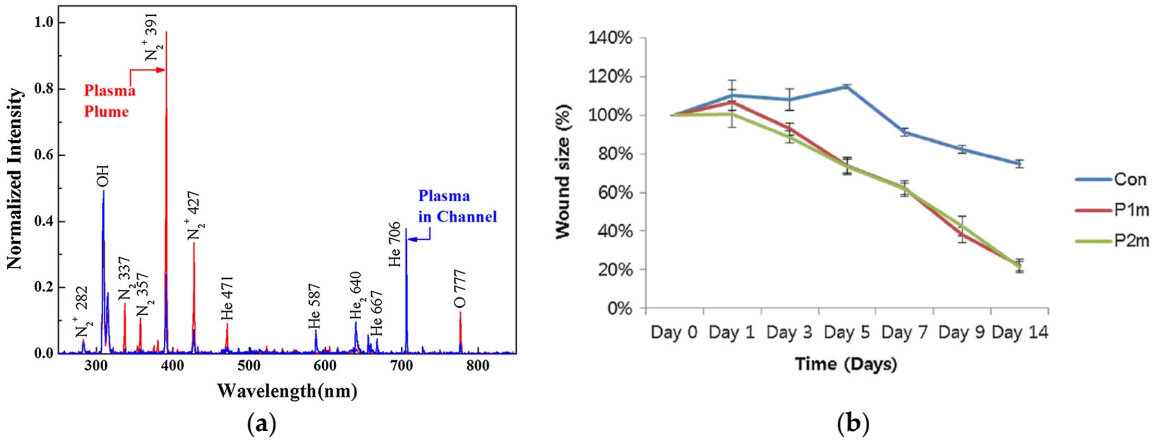

Figure 6. (**a**) Optical emission spectra corresponding to a 3 × 3 array microplasma jet measured in the channel and outside in open air. (**b**) Evaluation of burn closure times in rats after plasma jet treatment for 1 min (P1m) and 2 min (P2m) compared to a control sample (Con). Reprinted/adapted with permission from Ref. [41]. Copyright 2015, John Wiley & Sons, Ltd.

3.2. Low-Power Planar Uniform Jet Arrays

A compact device constituted by six independently actuated discharge cells has been reported by Li et al. [43]. The anode–cathode alternating arrangement was operated at an optimized electric field for argon flow. This setup yielded to discharges initiated at a breakdown voltage far below the Townsend potential. Such elementary discharges glowed in a non-self-sustained mode at relatively low voltages. Figure 7a,b shows the basic geometry features of one of the discharge devices of the so called "low-power large-scale uniform laminar plasma jet array". The parallel-connection arrangement of several of these cells was advantageous to send plasma jets with modulated V-I characteristics. Although the ceramic housing of the cells is not flexible, the APPJ striking from each individual anode–cathode segment can be independently sustained by the adequate combination of switches, so that the profile of electromagnetic irradiation and of reactive plasma species can be conveniently adapted to the specific sample topology.

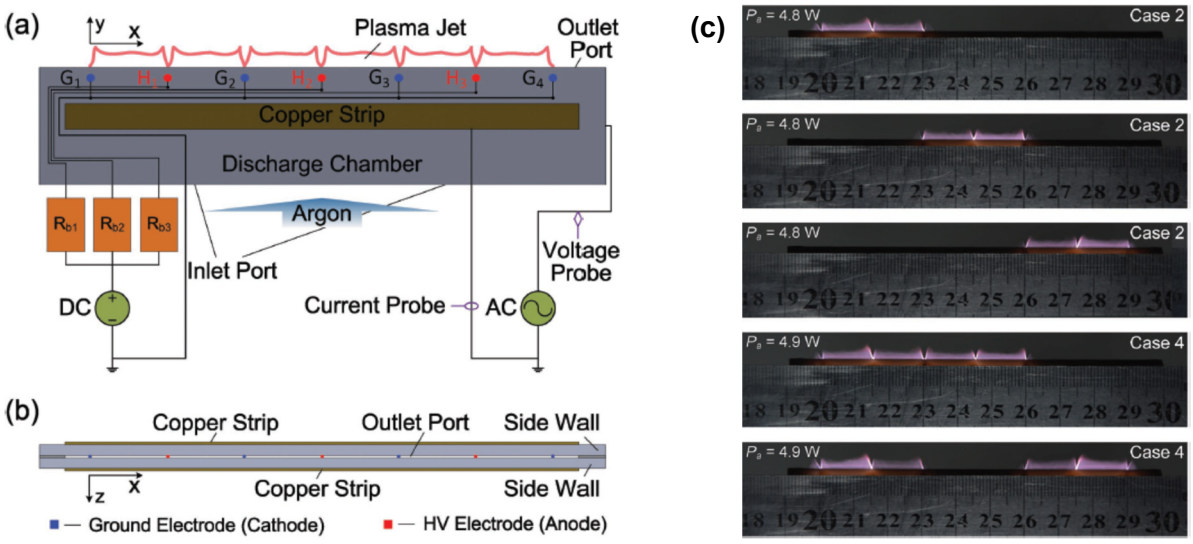

Figure 7. Sketch of a low-voltage laminar discharge array with plasma jets emanating from independently actuated cells. Each single discharge is controlled by actuating on separate switches. (**a**) Lateral, and (**b**) top view of the device. (**c**) Images of the planar jets striking in couples at different positions with similar values of input power. Reproduced from [43]. Published by Wiley-VCH under the Creative Commons CC BY license.

Figure 7c shows flexible arrangements to generate plasma jets using similar power values. The transverse light intensity emitted by the plasma array showed uniform profiles along each cell. In particular, configurations in groups of single, double, or quadruple stable plasma jets could be formed simultaneously by setting the adequate power distribution on an independent switch circuitry [43]. In this way, different zones of a sample surface can be selectively plasma-irradiated with the adequate switching arrangement at a low power cost. Although the impact of the discharge mode variation on RONS concentration has not been discussed, the basic plasma parameters, such as electron density, are expected to remain constant.

3.3. Deformable APPJ Platforms

Corbella et al. pioneered the use of bendable surfaces as multi-APPJ emitters [44,45]. Such pad-like sources are constituted by an array or matrices of one to five nozzles of millimeter size produced onto a silica aerogel foil. He plasmas were excited by 15 kHz-sinusoidal AC signals of around 10 kV peak-to-peak through Cu tape electrodes placed above and below the aerogel region. The spherical shaping of the nozzle aerogel surface provided voltage, current waveforms, and optical emission spectra qualitatively similar to the flat operation conditions. Therefore, the performance of the plasma multi-jet is not expected to vary upon the changes in the curvature state of the aerogel, which should correspond to the profile of the treated substrate in the final application. Figure 8 shows the multi-APPJ surface in operation in either concave or convex-shaping modes (curvature radius ≈ 5 mm). An OES analysis of the multi-jet provided the typical profile of emission lines dominated by nitrogen species, which come from the air mixed with the He jet column [46]. A jet divergence was clearly observed in flat and bent configurations, and it was attributed to electrostatic interactions between the plasma plumes [19].

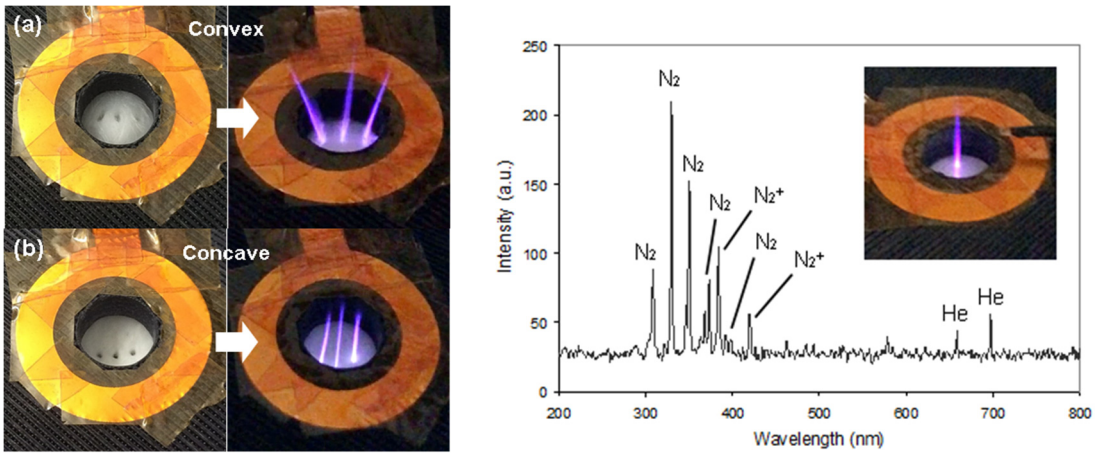

(**A**) (**B**)

Figure 8. (**A**) Photographs of the aerogel flexible array emitting three APPJs in convex (**a**) and concave (**b**) bending modes. The large aperture, which is 1 cm in diameter, is surrounded by a ring Cu tape acting as ground. (**B**) OES spectrum collected from the flat 3-plasma jet shown in the inset image. Reprinted/adapted with permission from Ref. [44]. Copyright 2021, Authors.

Power values limited to 5 W were obtained from the analysis of current and voltage waveforms of discharges corresponding to the 3-APPJ utilization. Since the power dissipated by the plasma plumes is a fraction of the total power consumed by the plasma source, i.e., DBD together with jets, such configuration may be adequate to build bendable plasma multi-jet prototypes to treat temperature-sensitive samples, such as biopolymers and organic tissues. Furthermore, upscaling the possibilities of this source should be tested by assembling multiple cells managed by independent power supplies.

Following up the study above, identical electric and gas feedings were applied to a low-density polyethylene (PE) cylindrical hollow housing to ignite APPJs in the radial direction [47]. The working principle is schematically shown in Figure 9. Briefly, a He flow was introduced in the axial direction of the cylinder cavity, which had mm-size radial channels through the walls. The electric field generated between an axial electrode rod and Cu tape glued around the outer perimeter was able to sustain the gas breakdown. The generated APPJs were produced from the He flow diverted from axial direction to radial direction in the laminar regime, and they showed electrical and optical behaviors comparable to the aerogel APPJ source described above. Although flexing tests of the hollow PE cylinder have not been reported to date, its soft and flexible consistency is promising for applications in which plasma jets need to reach delicate samples placed in locations of difficult access.

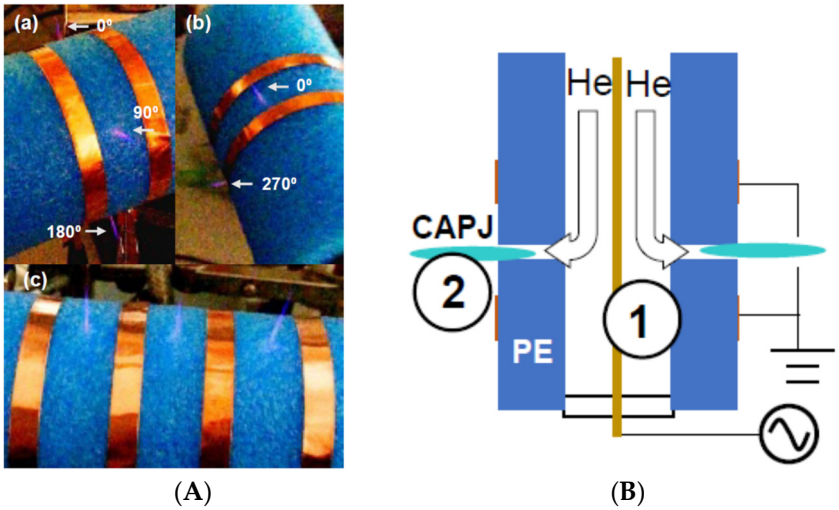

(**A**) (**B**)

Figure 9. (**A**) Images of the APPJ radial source in operation. Plasma jets are ignited from arrays either around the perimeter (**a**,**b**) or along the axial direction of the polyethylene (PE) cylinder (**c**). The cylinder has an outer diameter of 5.4 cm. (**B**) Scheme of the active DBD region (1) and the afterglow region (2) with the He cold atmospheric plasma jets (CAPJs). Reprinted/adapted with permission from Ref. [47]. Copyright 2021, Authors.

There are many possibilities to modify the cylindric source operation. For instance, the number of ejection holes can be increased if required. Simultaneously, the total flow rate should scale with the number of nozzles so that the flow regime does not change. The source can be also rotated around its axis to increase the treatment area and, additionally, to vary the plasma dose on the irradiated sample.

4. Flexible APPJ Channels

The necessity of treating locations of difficult access, such as in the case of surgical operations or endoscopic applications, motivated the development of APPJs produced along or at the end of flexible tubes [48,49]. The basic setup usually consists of a flexible tube or channel coupled to a DBD plasma source.

4.1. APPJ at Tube Exit

Despite the specific differences in the setups reported in the literature, such as tube length (a few centimeters up to a few meters) and biocompatible tube material (e.g., PVC and polyurethane), many prototypes involve a plastic tube lodging a thin floating Cu wire that prolongs from the DBD source up to a few millimeters before the tube ending (Figure 10a,b) [49–52]. In this way, the electrical power can be propagated to the exit of the tube in a transmission line fashion with negligible losses [52]. There is no plasma along the tube, and the APPJ restricted to the tip can remain near room temperature when operated

with the usual parameters (≈10 kV of AC voltage at ≈10 kHz) (Figure 10c). Otherwise, without a floating wire, the discharge would occupy the entire tube so that resources to prevent electroshock and plastic overheating would have to be in place [48].

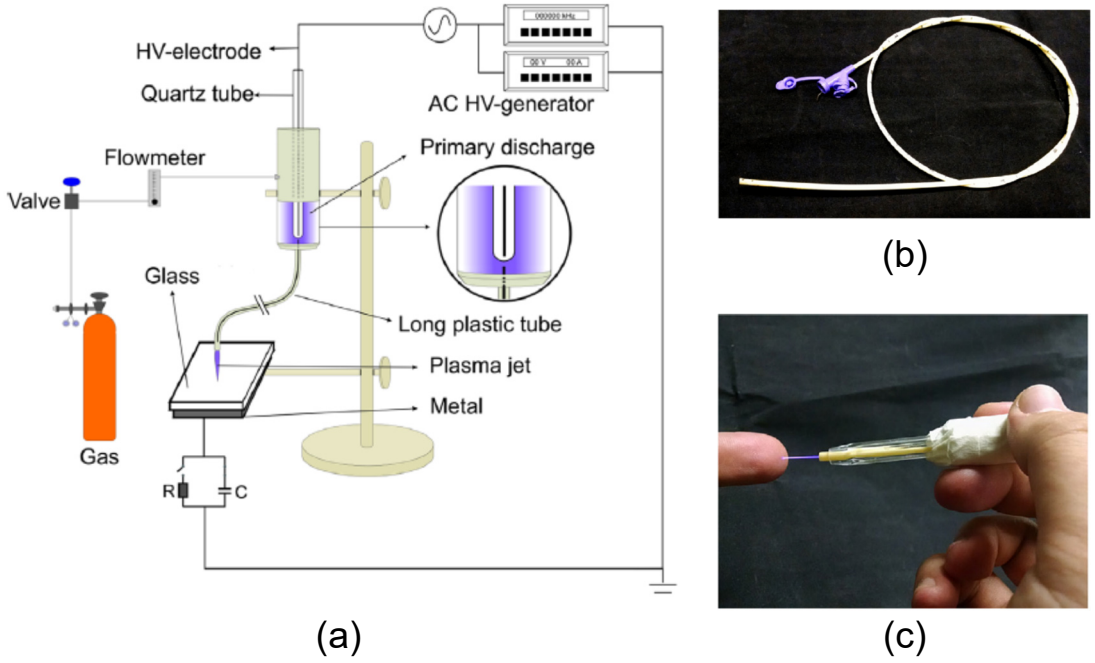

Figure 10. (**a**) Schematic layout of the flexible tube plasma source for microbial decontamination. A floating Cu wire within the tube shifts the plasma jet ignition to the very end. (**b**) Photo of a polyurethane nasogastric feeding tube used in the experiments. (**c**) APPJ emerging from the tip of a 1 m-plastic tube. Reprinted/adapted with permission from Ref. [50]. Copyright 2015, WILEY-VCH Verlag GmbH & Co.

Kostov et al. used an AC voltage input of 32 kHz modulated in 667 Hz-power bursts for a better control over the energy delivered to APPJ at the tube end [50]. Pulse duty cycle is around 20% of the low frequency. Hence, delicate samples, such as human skin or other tissues, may be treated without risk of overheating or burns thanks to a significant decrease in gas temperature. Naturally, the transient states of the discharge will affect the plasma parameters during treatment, and the specific frequency and duty cycle of the periodic signal are selected for each application. This approach has been adopted by other researchers working on long-tube APPJs for biomedical applications, especially for cancer therapy [53]. Figure 11 shows typical current and voltage waveforms at different timescales. The asymmetric shape of the current curve is due to the distinct streamer evolution during positive and negative voltage cycles.

A critical issue is the power loss in long dielectric tubes with inserted Cu wire. The transmission line model developed by Bastin et al. proved excellent to explain the high-frequency electromagnetic energy propagation along this system [52]. Power transmission efficiency is low in open-circuit conditions, i.e., when the APPJ strikes without target. In this case, leaks occur due to a capacitive coupling between the PTFE tube and atmosphere, as evidenced by the electric current decay measured along the tube. On the contrary, transmission efficiency is maximized in lines loaded with a solid conductive target, whose impedance is significantly lower than the jet impedance. The plume-target gap distance is another important variable for optimal power management.

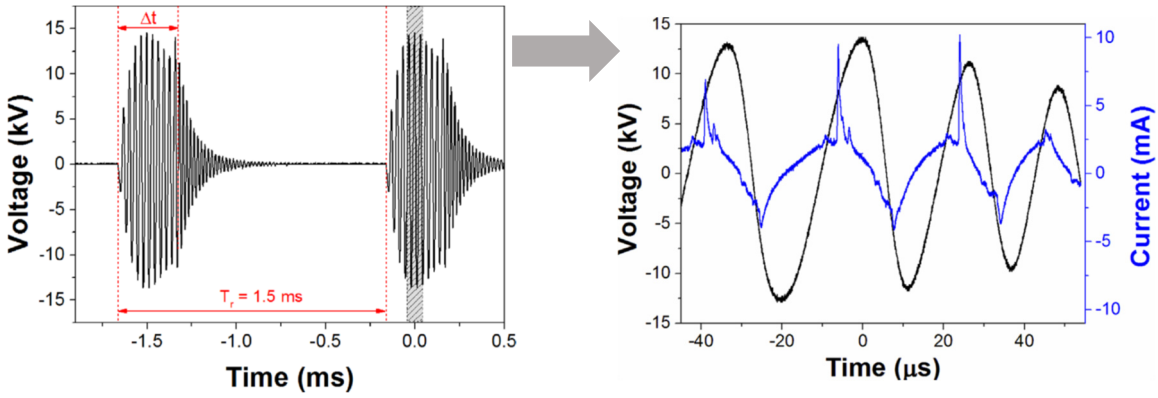

Figure 11. Waveform of the modulated voltage applied to a flexible capillary with inserted Cu wire. Plot followed by a detailed view of applied voltage and plasma currents signals measured in the time interval from the dashed rectangle. Reprinted/adapted with permission from Ref. [50]. Copyright 2015, WILEY-VCH Verlag GmbH & Co.

4.2. APPJ along Flexible Tube

In absence of metallic core wire, as for example in the use of dielectric capillaries with inner diameter < 1 mm, the APPJ discharge can fully occupy the inner volume of the tube. Such configuration has been successfully tested in clinical studies, for example, in the significant in vivo reduction in mice pancreatic tumor after plasma irradiation via flexible plasma gun [48]. Figure 12 shows an example of a plasma gun device filled with Ne discharge and a scheme of the DBD generator. In some applications, the tube can be coated with an Au thin film to act as an electrode and to shield UV radiation from plasma emission as well. Wang et al. demonstrated an excellent performance of such a coated APPJ channel after bending the capillary 200 times at −180° and 180° [54]. APPJs operated through capillary tubes must be fed by relatively small gas flow rates, namely of the order of 1 lpm or less, to keep a laminar flow regime.

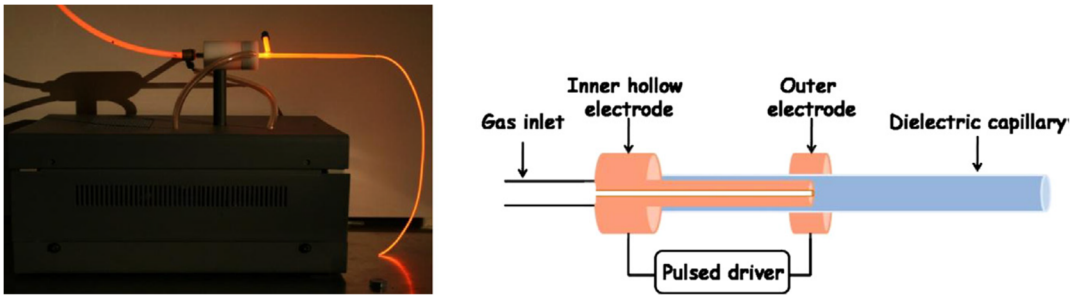

Figure 12. Plasma gun device filled with a neon discharge generated by DBD reactor. The discharge is ignited with a nanosecond pulse driver and leaves the DBD outlet through a 4 mm branched glass capillary, which is connected to a silicone capillary acting as an APPJ guide. Reprinted/adapted with permission from Ref. [48]. Copyright 2013, Elsevier GmbH.

Geng et al. explored further geometries of narrow flexible tubes acting as APPJ sources [55]. Different lengths and diameters of transparent Teflon tubes were adapted to the tested conditions of high and low values of nitrogen flow rate. Hence, a 10 cm tube was appropriate for 6 lpm, while a 120 cm tube enabled the transport at 18 lpm. To prevent gas-heating issues, a vortex tube was added between the electrode and gas supply systems to reduce the plasma jet temperature. Moreover, this APPJ system admits several architectural options intended for different applications. Figure 13 shows the flexible plasma jet system operating with different numbers of bifurcations and as a plasma jet brush (radial mode), the latter being an alternative to the radial APPJ source (hollow PE cylinder) discussed above [47]. The enhancement of the wettability of different materials

upon plasma irradiation validated the performance of the flexible plasma source to modify surface properties without structural degradation.

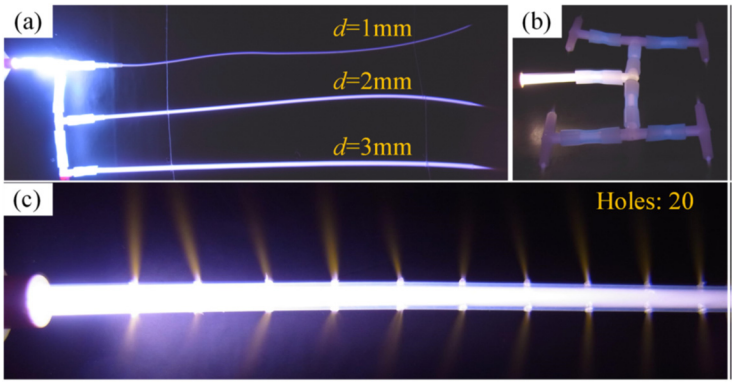

Figure 13. (**a**) Non-thermal plasma jets along flexible tubes branched with 3 bifurcations with different diameter values, *d*. (**b**) System with several bifurcations. (**c**) Plasma jet brush mode with 20 holes. Reprinted/adapted with permission from Ref. [55]. Copyright 2018, Authors.

It is difficult to predict the maximal length in flexible tubes still enabling an effective APPJ outcome given the number of experimental parameters involved, such as tube material and gas flow regime. However, a rough estimation on the order of magnitude can be made. Assuming a longest timescale of $t \approx 0.1$–1 s for plasma chemistry reactions and diffusion processes involving radicals and neutrals [56], a gas flow rate of 1 lpm, and a tube diameter of 1 mm (linear velocity $v \approx 20$ m/s), the theoretical maximal length is limited to $L = v \cdot t \approx 10$ m. This value is consistent with the reported APPJ tube devices. Additionally, a gradient in plasma optical emission is expected along the tube due to energy extinction. Therefore, the energy decay rate along the tube length can be monitored by OES analysis at different distances from the source.

5. Final Remarks

5.1. Summary and Discussion

Here, the state-of-the-art research in flexible APPJ source design, characterization, and applications has been briefly presented. The discussed prototypes show excellent advantages for many applications, namely room-temperature treatments; adaptation to large-area surfaces containing features such as asperities and microcavities; homogeneous irradiation with reactive neutrals and ions, and UV photons; and finally, the possibility of working at atmospheric pressure conditions. These properties make flexible jet sources unique for uniform plasma treatments without the inconveniences of vacuum pumping systems and scanning routines to ensure homogeneous plasma fluxes.

Table 1 summarizes the main approaches in the subjects of morphing APPJ sources, devices with independent APPJ nozzle operation, and plasma jets through flexible tubes. Although the list of references is not exhaustive, the cited works are representative of each type of plasma source.

The above results suggest that a milestone in the design and construction of a flexible multi-jet device could consist of a thin foil enclosing the necessary circuit elements and gas microchannels for an acceptable plasma outcome. Figure 14 sketches the basic concept of a multi-APPJ "shower" able to adapt its morphology to any sample shape. The corresponding plasma sources need to prove mechanically flexible, versatile, and efficient performances in surface treatments. For example, in the treatment of skin at body extremities, the plasma-operating parameters should be optimized so that the right dosages of plasma species reach out uniformly to the layer thicknesses of the epidermis (≈40 µm–1 mm), dermis (≈1 mm), and hypodermis (≈10 mm) [14]. Simultaneously, irradiation doses should lie within the tolerance margins to prevent skin damage.

Table 1. Morphing plasma jet sources and flexible APPJ nozzles together with their characteristics, operation parameters range and intended applications.

Source	Array	Gas/Power Supply	Applications	Refs.
Close-packed micro-APPJ	Silicone polymer Integrated rod electrodes 8 × 8 nozzles, 0.35 mm diam.	<5 lpm He 20 kHz, 1–100 mW	Wound healing Drinking-water treatment	[39–41]
Low-power planar discharge cells	Ceramic cells Activation by independent switching 6 cells, 0.5 × 15 mm^2/cell	<15 lpm Ar 8 kHz, 5–10 W/cell	Large and uniform plasmas	[43]
Flexible APPJ platforms	Silica aerogel (flat), PE (cylindric) External Cu tape electrodes 1–5 nozzles, 1 mm diam.	<10 lpm He 15 kHz, 0.1–5 W	Wound healing, surgical margins, and surface processing (proposed)	[44,45,47]
Flexible micro-APPJ tube	Silicone, Teflon Empty or coated tube 0.1–1 mm diam., a few meters long	<1 lpm He, Ne, Ar, N_2, +O_2 * 1–20 kHz, 1–20 kV	Plasma endoscopy Internal surface processing, machining	[48,54,55]
APPJ at the end of a flexible tube	PVC, PTFE Floating Cu wire >1 mm diam., <5 m-long	≈1 lpm He, Ar 5–20 kHz, 1–80 W	Plasma endoscopy Fungal deactivation	[49–53]

* O_2 was added to adjust the plasma chemistry.

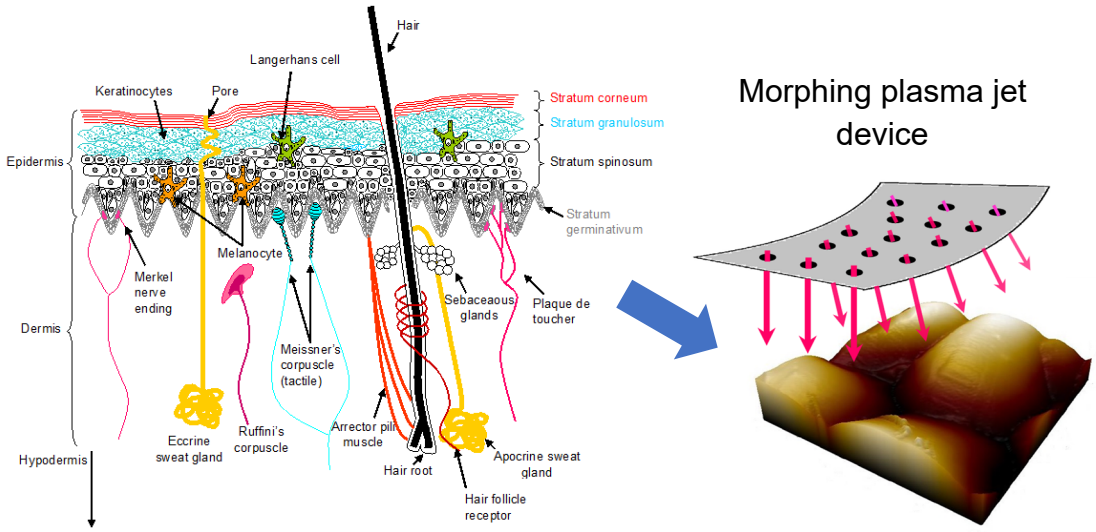

Figure 14. Drawing of skin cross section and schematic representation of a morphing plasma jet source treating a sample with irregular topography. Flexibility, versatility, and efficiency are crucial aspects in the APPJ source performance. In the treatment of skin, the plasma-operating parameters should be tuned considering the penetration depths of plasma species vs. layer thicknesses of epidermis (≈40 µm–1 mm), dermis (≈1 mm), and hypodermis (≈10 mm).

In fact, human skin constitutes an exceptional laboratory to test the performance of flexible APPJ prototypes for gentle healthcare treatments by mimicking complex topologies. The potentials of cold APPJs in cutaneous biology are numerous and well-adapted to this multiresponse organic tissue. APPJs can indeed exert their activity at different levels of the

skin; the length of penetration will promote different types of reaction depending on the treatment [14]. At the superficial level (epidermis), they promote hydration, acidification, and decontamination of the stratum corneum. Inside the skin (dermis and hypodermis) via APPJ-generated RONS, they can penetrate intercellularly (inter), intracellularly (intra) or in a transappendageal way (trans). They can promote the absorption of other molecules, such as drugs, by loosening the skin barrier. At the molecular and cellular level, in the skin (RONS), plasma jets can influence the oxidation of skin biomolecules, the activation of cellular metabolism, and signaling. Finally, at the tissue level, APPJs can increase cutaneous oxygenation, and stimulate vasculogenesis and the remodeling of the extracellular matrix.

Some of the main technological challenges to be addressed to get uniform plasma treatments of large, uneven areas by compact-morphing sources are mentioned below.

5.2. Outlook

The small number of articles published on the topic of flexible plasma jet sources for room-temperature treatments demonstrates the novelty of such technology. Nevertheless, here we speculate some future directions that research on flexible APPJ sources may take in the following years.

The next generation of non-equilibrium flexible plasma jet sources will demand the miniaturization of the driving setup for a more convenient device manipulation. Ongoing efforts involve the manufacturing of small-size piezo transformers to build more compact generators for portable plasma jet devices [57]. Recently, Liu et al. fabricated a 3D multi-microhole plasma jet instrument driven with nanosecond-pulsed power for underwater discharges [58]. Its layout could be applied to fabricate a miniaturized version of the soft cylindrical source aimed at plasma-liquid applications [47].

The development of flexible multi-jet headers for imprinting purposes opens a new field in lithography applications for non-flat surfaces, for instance, in the processing of third-generation photovoltaic systems and other microelectronic architectures [59]. Another interesting approach would be the production of diffuse, and laterally extended and uniform APPJs through porous flexible structures. Hong et al. and Ma et al. have studied the formation of diffuse APPJs through ceramics with open pores [60,61], and the next step will involve using a flexible analog to accommodate the porous structure to uneven profiles. An important challenge will be to maintain the processing performance upon the tensile and compressive stresses of the porous structure. Finally, to avoid the degradation of the treated samples, the gas temperature and electron density of the new APPJ devices should lie within the tolerances determined by the healthcare and food-processing regulations.

Flexible APPJ source prototypes have shown excellent performance so far, and they are promising for industrial steps in which surface modification of soft matter and biomaterials is a must.

Author Contributions: Conceptualization, M.K. and C.C.; methodology, C.C. and S.P.; investigation, C.C. and S.P.; resources, M.K., S.P. and C.C.; supervision, M.K.; writing—original draft preparation, C.C.; writing—review and editing, M.K. and S.P.; project administration, M.K. and C.C.; funding acquisition, M.K. All authors have read and agreed to the published version of the manuscript.

Funding: This research was partially supported by the National Science Foundation through Award No. 1919019.

Institutional Review Board Statement: Not applicable.

Informed Consent Statement: Not applicable.

Data Availability Statement: No new data were created or analyzed in this study.

Conflicts of Interest: The authors declare no conflict of interest.

References

1. Schütze, A.; Jeong, J.Y.; Babayan, S.E.; Park, J.Y.; Selwyn, G.S.; Hicks, R.F. The Atmospheric-Pressure Plasma Jet: A Review and Comparison to Other Plasma Sources. *IEEE Trans. Plasma Sci.* **1998**, *26*, 1685–1694. [CrossRef]
2. Viegas, P.; Slikboer, E.; Bonaventura, Z.; Guaitella, O.; Sobota, A.; Bourdon, A. Physics of plasma jets and interaction with surfaces: Review on modelling and experiments. *Plasma Sources Sci. Technol.* **2022**, *31*, 053001. [CrossRef]
3. Li, Q.; Pu, Y.-K.; Lieberman, M.A.; Economou, D.J. Dynamic model of streamer coupling for the homogeneity of glowlike dielectric barrier discharges at near-atmospheric pressure. *Phys. Rev. E* **2011**, *83*, 046405. [CrossRef] [PubMed]
4. Fridman, G.; Peddinghaus, M.; Ayan, H.; Fridman, A.; Balasubramanian, M.; Gutsol, A.; Brooks, A.; Friedman, G. Blood Coagulation and Living Tissue Sterilization by Floating-Electrode Dielectric Barrier Discharge in Air. *Plasma Chem. Plasma Process.* **2006**, *26*, 425–442. [CrossRef]
5. Graves, D.B. Low temperature plasma biomedicine: A tutorial review. *Phys. Plasma* **2014**, *21*, 080901. [CrossRef]
6. Laroussi, M. Plasma Medicine: A Brief Introduction. *Plasmas* **2018**, *1*, 47–60. [CrossRef]
7. Keidar, M.; Yan, D.; Sherman, J.H. *Cold Plasma Cancer Therapy*; Morgan & Claypool Publishers: San Rafael, CA, USA, 2019. [CrossRef]
8. Reuter, S.; von Woedtke, T.; Weltmann, K.-D. The kINPen-a review on physics and chemistry of the atmospheric pressure plasma jet and its applications. *J. Phys. D Appl. Phys.* **2018**, *51*, 233001. [CrossRef]
9. Xie, J.; Chen, Q.; Suresh, P.; Roy, S.; White, J.F.; Mazzeo, A.D. Paper-based plasma sanitizers. *PNAS* **2017**, *114*, 5119–5124. [CrossRef]
10. Kim, J.; Choi, K.-H.; Kim, Y.; Park, B.J.; Cho, G. Wearable Plasma Pads for Biomedical Applications. *Appl. Sci.* **2017**, *7*, 1308. [CrossRef]
11. Jung, H.; Seo, J.A.; Choi, S. Wearable Atmospheric Pressure Plasma Fabrics Produced by Knitting Flexible Wire Electrodes for the Decontamination of Chemical Warfare Agents. *Sci. Rep.* **2017**, *7*, 40746. [CrossRef]
12. Gershman, S.; Harreguy, M.B.; Yatom, S.; Raitses, Y.; Efthimion, P.; Haspel, G. A low power flexible dielectric barrier discharge disinfects surfaces and improves the action of hydrogen peroxide. *Sci. Rep.* **2021**, *11*, 4626. [CrossRef] [PubMed]
13. Lin, L.; Keidar, M. A map of control for cold atmospheric plasma jets: From physical mechanisms to optimizations. *Appl. Phys. Rev.* **2021**, *8*, 011306. [CrossRef]
14. Busco, G.; Robert, E.; Chettouh-Hammas, N.; Pouvesle, J.-M.; Grillon, C. The emerging potential of cold atmospheric plasma in skin biology. *Free Radic. Biol. Med.* **2020**, *161*, 290–304. [CrossRef] [PubMed]
15. Maho, T.; Damany, X.; Dozias, S.; Pouvesle, J.-M.; Robert, E. Atmospheric Pressure Multijet Plasma Sources For Cancer Treatments. *Clin. Plasma Med.* **2018**, *9*, 3–4. [CrossRef]
16. Babaeva, N.Y.; Kushner, M.J. Interaction of multiple atmospheric-pressure micro-plasma jets in small arrays: He/O_2 into humid air. *Plasma Sources Sci. Technol.* **2014**, *23*, 015007. [CrossRef]
17. Lietz, A.M.; Damany, X.; Robert, E.; Pouvesle, J.-M.; Kushner, M.J. Ionization wave propagation in an atmospheric pressure plasma multi-jet. *Plasma Sources Sci. Technol.* **2019**, *28*, 125009. [CrossRef]
18. Ghasemi, M.; Olszewski, P.; Bradley, J.W.; Walsh, J.L. Interaction of multiple plasma plumes in an atmospheric pressure plasma jet array. *J. Phys. D Appl. Phys.* **2013**, *46*, 052001. [CrossRef]
19. Wang, R.; Zhao, Y.; Zhang, S.; Zhang, P.; Zheng, S.; Shao, T. The Effect of Accumulated Charges and Fluid Dynamics on the Helium Plasma Jet Array Behavior. *IIIE Trans. Plasma Sci.* **2019**, *47*, 4861–4867. [CrossRef]
20. Liu, F.; Zhang, B.; Fang, Z.; Wan, M.; Wan, H.; Ostrikov, K. Jet-to-jet interactions in atmospheric-pressure plasma jet arrays for surface processing. *Plasma Process. Polym.* **2018**, *15*, 1700114. [CrossRef]
21. Martinez, L.; Dhruv, A.; Lin, L.; Balaras, E.; Keidar, M. Interaction between a helium atmospheric plasma jet and targets and dynamics of the interface. *Plasma Sources Sci. Technol.* **2019**, *28*, 115002. [CrossRef]
22. Viegas, P.; Slikboer, E.; Bonaventura, Z.; Garcia-Caurel, E.; Guaitella, O.; Sobota, A.; Bourdon, A. Quantification of surface charging memory effect in ionization wave dynamics. *Sci. Rep.* **2022**, *12*, 1181. [CrossRef] [PubMed]
23. Wan, M.; Liu, F.; Fang, Z.; Zhang, B.; Wan, H. Influence of gas flow and applied voltage on interaction of jets in a cross-field helium plasma jet array. *Phys. Plasma* **2017**, *24*, 093514. [CrossRef]
24. Xiong, R.; Xiong, Q.; Nikiforov, A.Y.; Vanraes, P.; Leys, C. Influence of helium mole fraction distribution on the properties of cold atmospheric pressure helium plasma jets. *J. Appl. Phys.* **2012**, *112*, 033305. [CrossRef]
25. Mericam-Bourdet, N.; Laroussi, M.; Begum, A.; Karakas, E. Experimental investigations of plasma bullets. *J. Phys. D Appl. Phys.* **2009**, *42*, 055207. [CrossRef]
26. Boeuf, J.-P.; Yang, L.L.; Pitchford, L.C. Dynamics of a guided streamer ('plasma bullet') in a helium jet in air at atmospheric pressure. *J. Phys. D Appl. Phys.* **2013**, *46*, 015201. [CrossRef]
27. Cho, G.; Kim, J.; Kang, H.; Kim, Y.; Kwon, G.-C.; Uhm, H.S. Electrical potential measurement in plasma columns of atmospheric plasma jets. *J. Appl. Phys.* **2012**, *112*, 103305. [CrossRef]
28. Fang, Z.; Ruan, C.; Shao, T.; Zhang, C. Two discharge modes in an atmospheric pressure plasma jet array in argon. *Plasma Sources Sci. Technol.* **2016**, *25*, 01LT01. [CrossRef]
29. Gorbanev, Y.; Golda, J.; Schulz-von der Gathen, V.; Bogaerts, A. Applications of the COST Plasma Jet: More than a Reference Standard. *Plasma* **2019**, *2*, 316–327. [CrossRef]

30. Reuter, R.; Rügner, K.; Ellerweg, D.; de los Arcos, T.; von Keudell, A.; Benedikt, J. The Role of Oxygen and Surface Reactions in the Deposition of Silicon Oxide like Films from HMDSO at Atmospheric Pressure. *Plasma Process. Polym.* **2012**, *9*, 1116–1124. [CrossRef]
31. Taghioskoui, M.; Zaghloul, M. U-Shaped Ultrahigh Frequency Atmospheric Pressure Plasma Jet With Magnetic Loop Antenna. *IEEE Trans. Plasma Sci.* **2017**, *45*, 43–53. [CrossRef]
32. Lin, L.; Pho, H.Q.; Zong, L.; Li, S.; Pourali, N.; Rebrov, E.; Tran, N.N.; Ostrikov, K.; Hessel, V. Microfluidic plasmas: Novel technique for chemistry and chemical engineering. *Chem. Eng. J.* **2021**, *417*, 129355. [CrossRef]
33. Castro, A.H.R.; Kostov, K.G.; Prysiazhnyi, V. Influence of Nozzle Shape on the performance of Low-Power Ar Plasma Jet. *IEEE Trans. Plasma Sci.* **2015**, *43*, 3228–3233. [CrossRef]
34. Mui, T.S.M.; Mota, R.P.; Quade, A.; Hein, L.R.O. Uniform surface modification of polyethylene terephthalate (PET) by atmospheric pressure plasma jet with a horn-like nozzle. *Surf. Coat. Technol.* **2018**, *352*, 338–347. [CrossRef]
35. Dobrynin, D.; Fridman, A. Planar He plasma jet: Plasma bullets formation, 2D bullets concept and imaging. *arXiv* **2018**, arXiv:1806.04626. [CrossRef]
36. Gugin, P.P.; Zakrevsky, D.E.; Milakhina, E.V. Investigation of a cold atmospheric plasma jet generation in single and multichannel planar devices. *J. Phys. Conf. Ser.* **2021**, *2064*, 012127. [CrossRef]
37. Weltmann, K.-D.; Fricke, K.; Stieber, M.; Brandenburg, R.; von Woedtke, T.; Schnabel, U. New Nonthermal Atmospheric-Pressure Plasma Sources for Decontamination of Human Extremities. *IEEE Trans. Plasma Sci.* **2012**, *40*, 2963–2969. [CrossRef]
38. Liu, B.; Qi, F.; Zhou, D.; Nie, L.; Xian, Y.; Lu, X. A novel flexible plasma array for large-area uniform treatment of an irregular surface. *Plasma Sci. Technol.* **2022**, *24*, 035403. [CrossRef]
39. Ma, J.H.; Shih, D.C.; Park, S.-J.; Eden, J.G. Microplasma Jets Generated by Arrays of Microchannels Fabricated in Flexible Molded Plastic. *IEEE Trans. Plasma Sci.* **2011**, *39*, 2700–2701. [CrossRef]
40. Sun, P.P.; Cho, J.H.; Park, C.-H.; Park, S.-J.; Eden, J.G. Close-Packed Arrays of Plasma Jets Emanating From Microchannels in a Transparent Polymer. *IEEE Trans. Plasma Sci.* **2012**, *40*, 2946–2950. [CrossRef]
41. Lee, O.J.; Ju, H.W.; Khang, G.; Sun, P.P.; Rivera, J.; Cho, J.H.; Park, S.-J.; Eden, J.G.; Park, C.H. An experimental burn wound-healing study of non-thermal atmospheric pressure microplasma jet arrays. *J. Tissue Eng. Regen. Med.* **2016**, *10*, 348–357. [CrossRef]
42. Sun, P.P.; Araud, E.M.; Huang, C.; Shen, Y.; Monroy, G.L.; Zhong, S.; Tong, Z.; Boppart, S.A.; Eden, J.G.; Nguyen, T.H. Disintegration of simulated drinking water biofilms with arrays of microchannel plasma jets. *NPJ Biofilms Microbiomes* **2018**, *4*, 24. [CrossRef] [PubMed]
43. Li, J.; Wang, J.; Lei, B.; Zhang, T.; Tang, J.; Wang, Y.; Zhao, W.; Duan, Y. A Highly Cost-Efficient Large-Scale Uniform Laminar Plasma Jet Array Enhanced by V-I Characteristic Modulation in a Non-Self-Sustained Atmospheric Discharge. *Adv. Sci.* **2020**, *7*, 1902616. [CrossRef] [PubMed]
44. Corbella, C.; Portal, S.; Lin, L.; Keidar, M. Non-thermal plasma multi-jet platform based on a flexible matrix. *Rev. Sci. Instrum.* **2021**, *92*, 083505. [CrossRef] [PubMed]
45. Corbella, C.; Portal, S.; Lin, L.; Keidar, M. Towards the fabrication of a morphing plasma source for biomedical applications. *arXiv* **2021**, arXiv:2102.02937. [CrossRef]
46. Thiyagarajan, M.; Sarani, A.; Nicula, C. Optical emission spectroscopic diagnostics of a non-thermal atmospheric pressure helium-oxygen plasma jet for biomedical applications. *J. Appl. Phys.* **2013**, *113*, 233302. [CrossRef]
47. Corbella, C.; Portal, S. Flexible plasma multi-jet source operated in radial discharge configuration. *Rev. Sci. Instrum.* **2021**, *92*, 123502. [CrossRef]
48. Robert, E.; Vandamme, M.; Brulle, L.; Lerondel, S.; Le Pape, A.; Sarron, V.; Ries, D.; Darny, T.; Dozias, S.; Collet, G.; et al. Perspectives of endoscopic plasma applications. *Clin. Plasma Med.* **2013**, *1*, 8–16. [CrossRef]
49. Kostov, K.G.; Machida, M.; Prysiazhnyi, V.; Honda, R.Y. Transfer of a cold atmospheric pressure plasma jet through a long flexible plastic tube. *Plasma Sources Sci. Technol.* **2015**, *24*, 025038. [CrossRef]
50. Kostov, K.G.; Nishime, T.M.C.; Machida, M.; Borges, A.C.; Prysiazhnyi, V.; Koga-Ito, C.Y. Study of Cold Atmospheric Plasma Jet at the End of Flexible Plastic Tube for Microbial Decontamination. *Plasma Process. Polym.* **2015**, *12*, 1383–1391. [CrossRef]
51. Bousba, H.E.; Sahli, S.; Namous, W.S.E.; Benterrouche, L. On the Stability and Turbulences of Atmospheric-Pressure Plasma Jet Extracted From the Exit of a Long Flexible PVC Tube. *IEEE Trans. Plasma Sci.* **2022**, *50*, 1218–1226. [CrossRef]
52. Bastin, O.; Thulliez, M.; Servais, J.; Nonclercq, A.; Delchambre, A.; Hadefi, A.; Deviere, J.; Reniers, F. Optical and Electrical Characteristics of an Endoscopic DBD Plasma Jet. *Plasma Med.* **2020**, *10*, 71–90. [CrossRef]
53. Binenbaum, Y.; Ben-David, G.; Gil, Z.; Slutsker, Y.Z.; Ryzhkov, M.A.; Felsteiner, J.; Krasik, Y.E.; Cohen, J.T. Cold Atmospheric Plasma, Created at the Tip of an Elongated Flexible Capillary Using Low Electric Current, Can Slow the Progression of Melanoma. *PLoS ONE* **2017**, *12*, e0169457. [CrossRef]
54. Wang, T.; Wang, J.; Wang, S.; Chen, S.; Wang, X.; Yang, W.; Li, M.; Shi, L. Atmospheric micro-sized cold plasma jet created by a long and ultra-flexible generator with sputtered gold thin film electrode. *J. Micromech. Microeng.* **2022**, *32*, 095006. [CrossRef]
55. Geng, J.; Yin, S.; Huang, S.; Tang, Q.; Luo, H.; Chen, F. Flexible cold plasma jet with controllable length and temperature for hydrophilic modification. *Phys. Plasma* **2018**, *25*, 083508. [CrossRef]
56. Park, S.; Choe, W.; Moon, S.Y.; Yoo, S.J. Electron characterization in weakly ionized collisional plasmas: From principles to techniques. *Adv. Phys. X* **2019**, *4*, 1526114. [CrossRef]

57. Johnson, M.J.; Boris, D.R.; Petrova, T.B.; Walton, S.G. Characterization of a Compact, Low-Cost Atmospheric-Pressure Plasma Jet Driven by a Piezoelectric Transformer. *IEEE Trans. Plasma Sci.* **2019**, *47*, 434–444. [CrossRef]
58. Liu, Z.; Wang, S.; Pang, B.; Gao, Y.; Li, Q.; Xu, D.; Liu, D.; Zhou, R. A novel designed 3D multi-microhole plasma jet device driven by nanosecond pulse at atmospheric pressure. *Plasma Sources Sci. Technol.* **2022**, *31*, 05LT03. [CrossRef]
59. Mariotti, D.; Belmonte, T.; Benedikt, J.; Velusamy, T.; Jain, G.; Svrcek, V. Low-Temperature Atmospheric Pressure Plasma Processes for "Green" Third Generation Photovoltaics. *Plasma Process. Polym.* **2016**, *13*, 70–90. [CrossRef]
60. Hong, Y.C.; Yoo, S.R.; Lee, B.J. An atmospheric-pressure nitrogen-plasma jet produced from microdischarges in a porous dielectric. *J. Electrostat.* **2011**, *69*, 92–96. [CrossRef]
61. Ma, S.H.; Kim, K.G.; Lee, S.J.; Moon, S.Y.; Hong, Y.C. Effects of a porous dielectric in atmospheric-pressure plasma jets submerged in water. *Phys. Plasma* **2018**, *25*, 083519. [CrossRef]